

# Catalytic ozonation process using modified activated carbon as a catalyst for the removal of sarafloxacin antibiotic from aqueous solutions

Maryam Dolatabadi <sup>a, b</sup>, and Saeid Ahmadzadeh <sup>c, d, \*</sup>

<sup>a</sup> student Research Committee, Kerman University of Medical Sciences, Kerman, Iran.

<sup>b</sup> Environmental Science and Technology Research Center, Department of Environmental Health Engineering, School of Public Health, Shahid Sadoughi University of Medical Sciences, Yazd, Iran.

<sup>c</sup> Pharmaceutics Research Center, Institute of Neuropharmacology, Kerman University of Medical Sciences, Kerman, Iran.

<sup>d</sup> Pharmaceutical Sciences and Cosmetic Products Research Center, Kerman University of Medical Sciences, Kerman, Iran

## ARTICLE INFO:

Received 2 Mar 2023

Revised form 5 May 2023

Accepted 29 May 2023

Available online 30 Jun 2023

## Keywords:

Sarafloxacin,  
 Catalytic ozonation,  
 Modified activated carbon,  
 Removal,  
 UV-Vis spectrometer,  
 Aqueous solution.

## ABSTRACT

Sarafloxacin (SAR) is an antibiotic from the fluoroquinolone group and is also one of the most widely used antibiotics in veterinary medicine. Potential performance and appropriate effectiveness have made SAR a special place among antibiotics. Antibiotic residues in the environment cause many problems, the most important of which is antibiotic resistance. Therefore, it is necessary to remove antibiotic residues from the environment. Response surface methodology (RSM) was utilized as a mathematics and statistics approach to optimize the removal efficiency of SAR using the catalytic ozonation process. The obtained regression equation for the response was the quadratic mathematical model. The coefficient of determination ( $R^2$ ), adjusted  $R^2$ , and predicted  $R^2$  were obtained at 0.9939, 0.9917, and 0.9855, respectively. The maximum removal efficiency of 99.3% was obtained under optimum conditions, including a SAR concentration of 30.0 mg L<sup>-1</sup>, ozone dose of 1.5 mg min<sup>-1</sup>, catalyst dose (modified activated carbon) of 600 mg L<sup>-1</sup>, pH of 5.0, and reaction time of 30 min. According to the obtained results, the catalytic ozonation process as a suitable technique can efficiently remove SAR and other pharmaceutical compounds.

## 1. Introduction

Sarafloxacin (SAR) is one of the most important synthetic antibiotics from the fluoroquinolone (FQs) group, which is widely used in human and veterinary medicine [1]. SAR works by inhibiting the activity of DNA gyrase and is still commonly used in poultry production, fish breeding, inhibiting fungal growth, and treatment of various diseases in aquatic animals, including eye protrusion, skin wounds, fin and tail rot, abdominal swelling, moreover, SAR is

used to treat mastitis, which is a common disease among animals and also to increase lactation and growth in livestock [2, 3]. Residues of antibiotics in the environment, especially aquatic ecosystems, are considered pollutants due to their adverse effects on humans, animals, and the environment. Toxicity, bacterial resistance, endocrine disorders, mutagenicity, and disturbance in the photosynthesis process of aquatic plants, are among the problems caused by the presence of residues of antibiotics in environments [4-6]. Residuals of FQs have been detected at levels of up to 0.45 and 0.036 μg L<sup>-1</sup> in wastewater and surface water, respectively [7, 8]. Although the concentration of residue

\*Corresponding Author: [Saeid Ahmadzadeh](mailto:Saeid.Ahmadzadeh@kmu.ac.ir)

Email: [chem\\_ahmadzadeh@yahoo.com](mailto:chem_ahmadzadeh@yahoo.com)

<https://doi.org/10.24200/amecj.v6.i02.236>

antibiotics in aquatic environments is low, their entry continuously causes concentration to accumulate, which is considered a potential risk in the long term. Moreover, the residues of some antibiotics in low concentrations cause many problems [9]. Therefore, it is necessary to remove antibiotic residues from aquatic environments. So far, several techniques have been used to remove residual antibiotics from aqueous media such as the process of adsorption [10-12], coagulation [13, 14], activated sludge [15], filtration [16-18], and advanced oxidation [19-21]. Ozonation is one of the advanced oxidation processes (AOPs) in water and wastewater treatment. The ozonation process alone often leads to low efficiency in mineralization. However, the removal efficiency by combining the ozonation process with other oxidation agents (UV or H<sub>2</sub>O<sub>2</sub>) can be improved but may increase the treatment and operation costs. In recent years, catalytic ozonation has attracted the attention of many researchers due to its high oxidation potential in water and wastewater treatment. Activated carbon (AC), an inexpensive material, was widely used as an adsorbent for organic and inorganic molecule removal in water and wastewater treatment [22]. Ozonation catalyzed by AC was reported to produce H<sub>2</sub>O<sub>2</sub> via the reaction of O<sub>3</sub> to the surface of AC, eventually resulting in ·OH formation, and active O·(s) species resulting from O<sub>3</sub> decomposition on AC surfaces. Pyrrol groups on ACs have been reported to increase the formation of O<sub>2</sub>·, resulting in ·OH formation and increased pollutant removal. AC can simultaneously adsorb a wide variety of pollutants because of its large surface area and porosity, whereas its reaction with ozone on its basic surface promotes strong oxidants that enable the mineralization of organic pollutants [23, 24].

According to the studies and knowledge of the research team, this is the first time the catalytic ozonation process using modified activated carbon as the catalyst for the removal of SAR antibiotic from aqueous solutions using CCD in response surface methodology (RSM) has been from aqueous solutions. The aims of this study are as follows:

(I) to investigate the effects of various operating parameters, such as the initial SAR concentration, ozone dose, and catalyst dosage (activated carbon), and (II) to optimize the SAR removal efficiency and investigate the main, interaction, and cubic effects of critical operating parameters.

## 2. Material and methods

### 2.1. Chemical

Sarafloxacin (C<sub>20</sub>H<sub>17</sub>F<sub>2</sub>N<sub>3</sub>O<sub>3</sub>) was purchased from Darou Pakhsh Pharmaceutical Company, Iran. NaOH (sodium hydroxide, CAS N.: 1310-73-2), KI (potassium iodide, CAS N.: 7681-11-0), HNO<sub>3</sub> (nitric acid, CAS N.: 7697-37-2), H<sub>2</sub>O<sub>2</sub> (hydrogen peroxide 30% (%w/w), CAS N.: 7722-84-1), HCl (hydrochloric acid, CAS N.: 100317), and activated charcoal (CAS N.: 7440-44-0) were obtained from Merck Co. All chemicals were of analytical reagent grade.

### 2.2. Catalytic ozonation process system

The catalytic ozonation of SAR was performed in a 500 mL Pyrex reactor with an 8.0 cm diameter and 12 cm high and equipped with a magnetic stirrer. Ozone was generated from the air using an ozone generator (ARDA, Model MOG+10) with an input rate of 5 g h<sup>-1</sup>. The reactor included an input/output port for the ozone gas stream. Ozone was introduced through a porous fritted diffuser that can produce reasonably fine bubbles. All experiments were performed at the ambient temperature (20±2 °C), constant pH of 5.0 ±0.5, and reaction time of 30 min. After performing the reaction in each experimental run, the concentration of SAR was measured at 272 nm using a UV-Vis spectrometer (OPTIZEN 3220 model).

### 2.3. Modification of activated carbon by MgCl<sub>2</sub> as catalyst

10.0 mg of commercial activated carbon (CAC) was mixed with 200 mL of 2.0 mM nitric acid for 3.0 h at 80 °C to convert to the hydrophilic form. After the mentioned time, the CAC particles were filtered and washed several times with distilled water to stabilize the pH and then dried at 110 °C.

Subsequently, 5.0 g of CAC from the previous step was added to 200 mL of  $MgCl_2$  10.0 mM and shaken for 24 h at room temperature. The thermal modification was carried out at 800 °C for 2.0 h under the  $N_2$  gas stream. Then, the modified CAC (MAC) was brought to ambient temperature and used as a catalyst in the catalytic ozonation process.

#### 2.4. Application of Response Surface Methodology

Response surface methodology (RSM) is a widely used mathematical and statistical approach employed to model, design, and evaluate the relationship between several independent variables and responses of the proposed model [25, 26]. Unlike conventional methods for data analysis, RSM analyzes data using simple techniques based on the mathematical model. In the RSM, to optimize the variables, a polynomial function (often a quadratic polynomial model) can be used, as given in Equation 1 [27-29].

$$Y = \beta_0 + \sum_{i=1}^k \beta_i X_i + \sum_{i=1}^k \beta_{ii} X_i^2 + \sum_{i=1}^{k-1} \sum_{j=i+1}^k \beta_{ij} X_i X_j + \varepsilon \quad (\text{Eq.1})$$

Where Y is the predicted response (SAR removal %), k is the number of independent factors,  $\beta_0$ ,  $\beta_i$ ,  $\beta_{ii}$ , and  $\beta_{ij}$  are the constant, linear, quadratic, and interaction model coefficients, respectively, also,  $X_i$ ,  $X_j$ , and  $\varepsilon$  are the independent factors and the error. Table 1 shows the ranges and levels of the studied variables [30].

The effect of the model, main, interaction and quadratic variables were investigated using analysis of variance (ANOVA) tools which included the *p*-value (probability value) and the *F*-value

(Fischer's test value). Furthermore, the parameter of regression analysis such as the determination coefficient ( $R^2$ ), adjusted  $R^2$  (Adj.  $R^2$ ), and predicted  $R^2$  (Pred.  $R^2$ ), were investigated [31, 32].

### 3. Result and Discussion

#### 3.1. Response surface methodology and results analysis

Table 2 shows the central composite design (CCD) matrix and the obtained results from each experimental run.

The adequacy and statistical evaluation of the significant variables for the predicted model were investigated using ANOVA. The obtained results of ANOVA are listed in Table 3.

$X_1$ ,  $X_2$ , and  $X_3$  are SAR concentration, ozone dose, and catalyst dosage. Also,  $X_2^2$  and  $X_3^2$  are the quadratic effects of ozone dose and catalyst dosage, respectively. According to the table.3, the model is significant due to the high *F*-value and *p*-value of less than 0.05. The *p*-values  $\leq 0.05$  indicate that model terms including  $X_1$ ,  $X_2$ ,  $X_3$ ,  $X_2^2$  and  $X_3^2$  are significant ( $X_2^2$ ). The *p*-value of lack of fit was 0.1111 (*p*-value less than 0.05, not significant), which indicates a good fit for the experimental data.

#### 3.2. diagnostic plots and adequacy check of the predicted model

Several diagnostic plots to prove the normality of data were analyzed. Diagnostic plots studied include normal plots of residuals, residuals vs. predicted, predicted vs. actual, and residuals vs. run. The normal plot of residuals and residuals versus the predicted plot is shown in Figure 1.

Table 1. Input factors and experimental levels of study

Coded Variables ( $X_i$ )	Factors	Experimental Field				
		- $\alpha$	-1	0	+1	+ $\alpha$
$X_1$	A= SAR concentration (mg L <sup>-1</sup> )	10	25	50	85	100
$X_2$	B= Ozone dose (mg min <sup>-1</sup> )	0.5	0.75	1.25	1.75	2.0
$X_3$	C= Catalyst dosage (mg L <sup>-1</sup> )	200	300	500	700	800

**Table 2.** Central composite design (CCD) matrix and experimental response

Run	Actual values			Coded values			Removal (%)
	A (mg L <sup>-1</sup> )	B (mg min <sup>-1</sup> )	C (mg L <sup>-1</sup> )	X <sub>1</sub>	X <sub>2</sub>	X <sub>3</sub>	
1	55	1.25	200	0	0	-1.5	73.4
2	55	1.25	500	0	0	0	88.7
3	55	1.25	800	0	0	1.5	87.1
4	25	1.75	300	-1	1	-1	85.3
5	100	1.25	500	1.5	0	0	79.4
6	85	0.75	700	1	-1	1	73.2
7	85	1.75	300	1	1	-1	71.8
8	25	0.75	300	-1	-1	-1	80.0
9	25	1.75	700	-1	1	1	96.4
10	55	1.25	500	0	0	0	90.1
11	55	1.25	500	0	0	0	89.1
12	10	1.25	500	-1.5	0	0	99.3
13	55	1.25	500	0	0	0	88.6
14	55	1.25	500	0	0	0	89.2
15	55	2.00	500	0	1.5	0	84.3
16	55	0.5	500	0	-1.5	0	71.1
17	55	1.25	500	0	0	0	89.4
18	85	0.75	300	1	-1	-1	63.6
19	25	0.75	700	-1	-1	1	89.2
20	85	1.75	700	1	1	1	80.9

**Table 3.** Analysis of variance (ANOVA) for the predicted model

Source	Sum of squares	Degree of freedom (df)	mean squares	F-Value	Probability P-value > F
Model	1581.5	5	316.3	455.0	< 0.0001
X <sub>1</sub>	666.1	1	666.1	958.2	< 0.0001
X <sub>2</sub>	185.8	1	185.8	267.3	< 0.0001
X <sub>3</sub>	283.7	1	283.7	408.1	< 0.0001
X <sub>2</sub> <sup>2</sup>	272.4	1	272.4	391.8	< 0.0001
X <sub>2</sub> <sup>2</sup>	165.5	1	165.5	238.3	< 0.0001
Residual	9.73	14	0.70	-	-
Lack of Fit	8.26	9	0.92	3.13	0.1111
Pure Error	1.47	5	0.29	-	-
Cor Total	1591.2	19	-	-	-

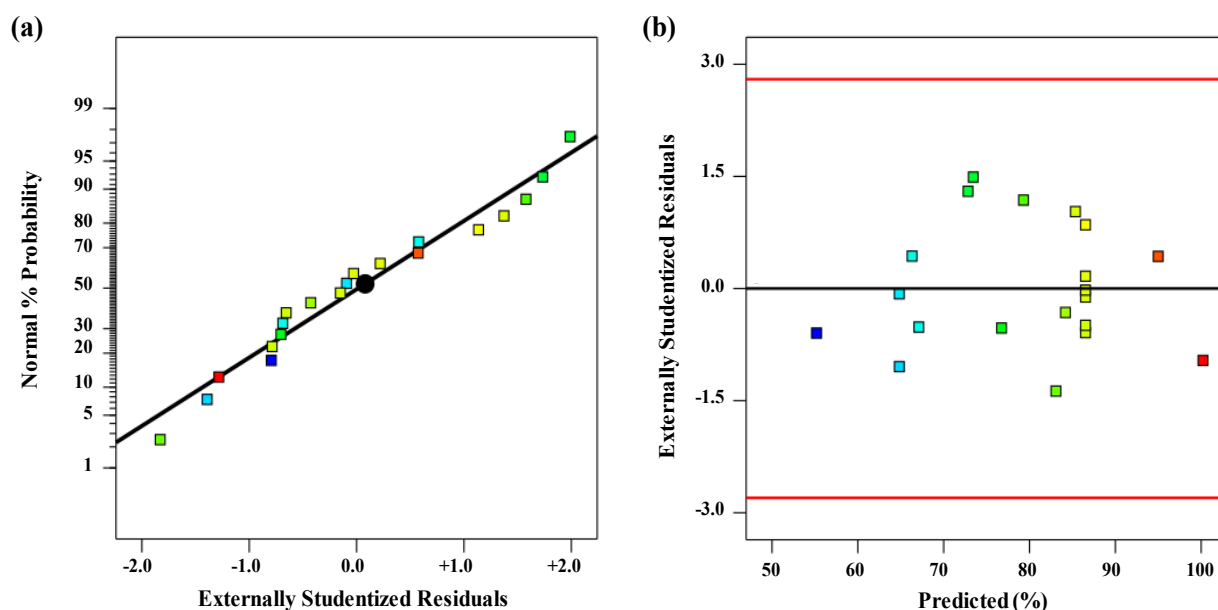


**Fig. 1.** Diagnostic plots (a) normal % probability *versus* externally studentized residuals, (b) Externally studentized residuals *versus* predicted

According to the results obtained from the diagnostic plots, the response showed a good fit, and all the points fall along the straight line and the specified lines. Consequently, the experimental data are in good agreement with the predicted model and confirm the normality of the data. The predicted versus actual and residuals versus run number plots are presented in Figure 2.

The  $R^2$  of the predicted model was 0.9939, indicating that 99.39% of the total variations in the results could be due to significant factors. Moreover, the Adj.  $R^2$  was 0.9917, which Adj.  $R^2$  was very close to  $R^2$ . Additionally, the difference between the Adj.  $R^2$  (0.9917) and pred.  $R^2$  (0.9855) is less than 0.2 [33, 34].

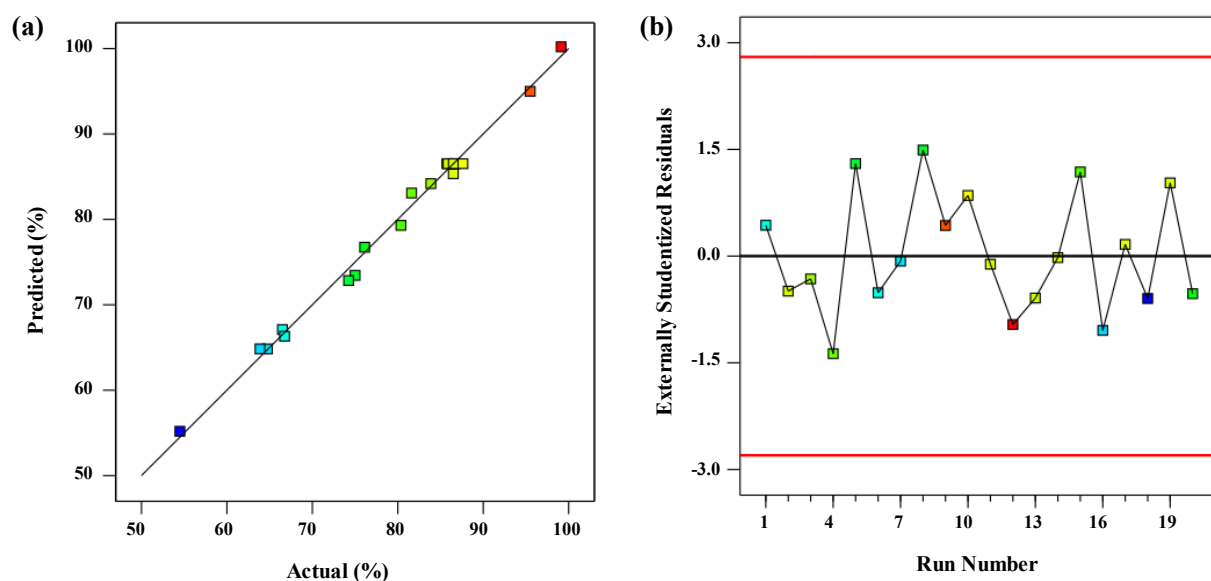


**Fig. 2.** Diagnostic plots (a) predicted *versus* actual, (b) Externally studentized residuals *versus* the run number

### 3.3. Predicted model and effect of variables

The predicted model can be expressed in coded units as Equation 2.

$$Y(\%) = 89.29 - 7.30X_1 + 3.86X_2 + 4.76X_3 - 5.14X_2^2 - 4.01X_3^2$$

(Eq.2)

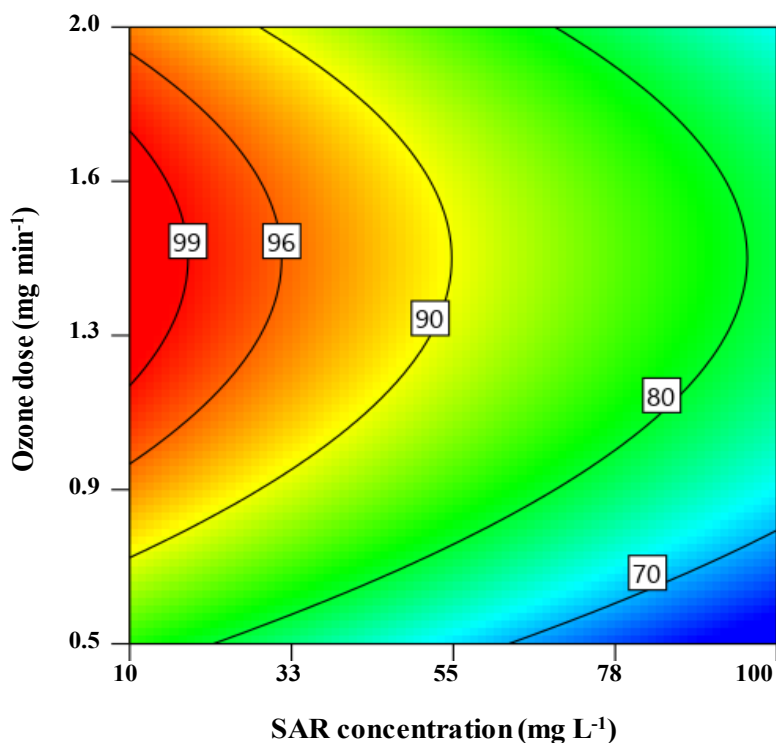
Y is the predicted response (SAR removal efficiency %),  $X_1$ ,  $X_2$ , and  $X_3$  are SAR concentration, ozone dose, and catalyst dosage. Also,  $X_2^2$  and  $X_3^2$  are the quadratic effects of ozone dose and catalyst dosage, respectively.

Figure 3 shows the contour plot of the effects of SAR concentration and ozone dose on SAR removal efficiency.

According to Figure 3, SAR concentration increases from 10 to 100 mg L<sup>-1</sup>, and the SAR removal efficiency decreases from 100% to 78.3% in the constant condition (ozone dose of 1.25 mg min<sup>-1</sup>, and catalyst dosage of 500 mg L<sup>-1</sup>). As can be seen in the predicted model, the SAR concentration ( $X_1$ ) has shown a negative sign (-7.30), which indicates the inverse effect on the

removal efficiency. The negative effect of SAR concentration on the removal efficiency during the catalytic ozonation process can be attributed to the phenomenon that when ozone dose and catalyst dosage be considered fixed, the number of radicals generated is constant. Only a specific amount of SAR molecules were degraded and by increasing SAR concentration there are not enough radical species in the reactor for the degradation of SAR molecules. Therefore, the SAR removal efficiency decreases [35, 36].

Figure 3 also shows the effect of the ozone dose on removal SAR efficiency. As the ozone dose increases from 0.5 to 2.0 mg min<sup>-1</sup>, the SAR removal efficiency increases from 71.8% to 83.4% in the constant condition (SAR concentration 55.0 mg L<sup>-1</sup>, and catalyst dosage 500 mg L<sup>-1</sup>). As can be seen in the predicted model, the ozone dose ( $X_2$ ) has shown a positive sign (+3.86), which indicates a positive effect on the SAR removal efficiency. According to Figure 3, the effect of the ozone dose has specified as a curve. Moreover, in the predicted model, the quadratic effect of the ozone dose ( $X_2^2$ )



**Fig.3.** Contour plot as a function of ozone dose and SAR concentration (Experimental conditions: catalyst dosage of 500 mg L<sup>-1</sup> pH of 5.0, and reaction time of 30 min)



is significant. When a variable has a significant quadratic effect, its effect will be shown as a curve, the increasing trend of ozone dose decreases after the concentration of 1.5, and the maximum SAR removal efficiency at the dosage of 1.5 is equal to 90.1%.

According to Figure 3, the effect of the ozone dose has specified as a curve. Moreover, in the predicted model, the quadratic effect of the ozone dose ( $X_2^2$ ) is significant. When a variable has a significant quadratic effect, its effect will be shown as a curve, the increasing trend of ozone dose decreases after the concentration of 1.5, and the maximum SAR removal efficiency at the dosage of 1.5 is equal to 90.1%. The reason for the increase in SAR removal efficiency by increasing the ozone dose can be because in the conditions where the SAR concentration and the dosage of catalyst are constant, with the increase in the ozone dose, the generation of radical species in the reactor also increases and as a result, the more number SAR molecules

are exposed to radical species and decompose, and subsequently the SAR removal efficiency increases [37, 38].

Figure 4 shows the 3D plot of the effects of the catalyst dosage and SAR concentration on the SAR removal efficiency.

As catalyst dosage increases from 200 to 800 mg L<sup>-1</sup>, the SAR removal efficiency increases from 73.1% to 87.3% in the constant condition (SAR concentration of 55.0 mg L<sup>-1</sup> and ozone dose of 1.25 mg min<sup>-1</sup>). As can be seen in Equation 2 (predicted model), the catalyst dosage ( $X_3$ ) has shown a positive sign (+4.76), which indicates a positive effect on the SAR removal efficiency. Furthermore, the quadratic effect of the catalyst dosage ( $X_3^2$ ) with a negative sign (-4.01) is also significant. The maximum SAR removal efficiency was obtained in the range of 600 to 700 mg L<sup>-1</sup> from the catalyst dosage. Catalysts create a synergistic effect on the decomposition of ozone molecules into other active radical species, and therefore the pollutants are decomposed faster [39].

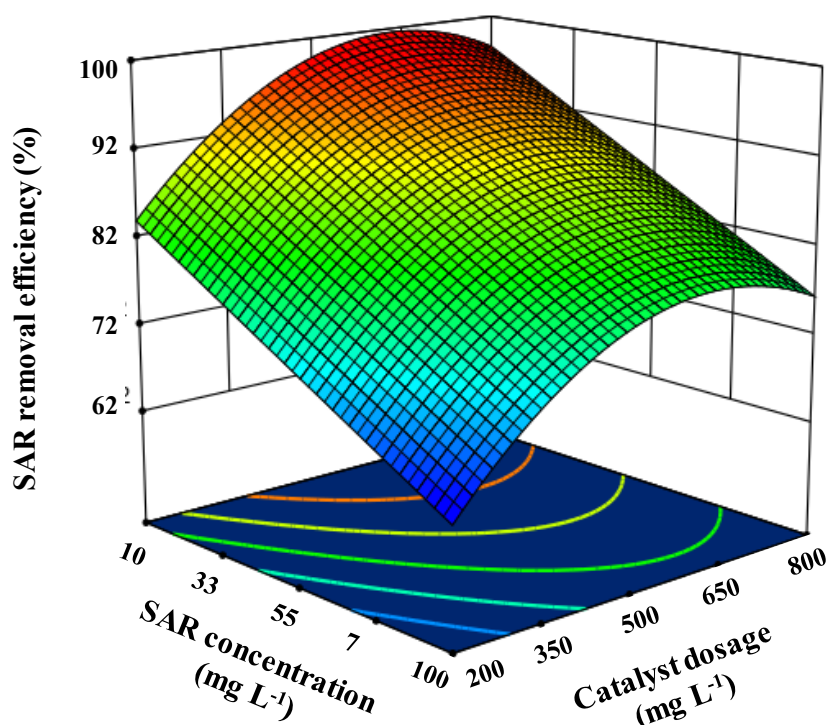


Fig. 4. 3D surface plot as a function of SAR concentration and catalyst dosage (Experimental conditions: ozone dose of 1.25 mg min<sup>-1</sup>, pH of 5.0, and reaction time of 30 min)

#### 4. Conclusion

Central composite design (CCD) optimized the SAR removal using a catalytic ozonation process. The main variables include the SAR concentration (10-100 mg L<sup>-1</sup>), ozone dose (0.5-2.0 mg min<sup>-1</sup>), and catalyst dosage (200-800 mg L<sup>-1</sup>). The effects of operating parameters including SAR concentration, ozone dose, and catalyst dose for SAR removal were studied using analysis of variance (ANOVA) and regression analysis. The predicted model confirmed that the predicted value agrees with the actual value. Modified AC by MgCl<sub>2</sub> (MAC) promoted ozone decomposition into reactive oxidizing species. The maximum SAR removal efficiency of 99.3% was achieved under optimal conditions. During the catalytic ozonation process; active free radicals are generated, increasing the degradation rate and mineralization of pollutants. Catalytic ozonation using MAC as a catalyst enhances the removal of more oxidized and saturated compounds.

#### 5. Acknowledgements

The authors would like to thank the student research committee of Kerman University of Medical Sciences [Grant number 401000073] for supporting the current work. This work received a grant from the Kerman University of Medical Sciences.

#### 6. Conflict of interest and Ethical approval

The authors declare that they have no conflict of interest regarding the publication of the current paper. The Ethics Committee of Kerman University of Medical Sciences approved the study (IR.KMU.REC.1401.098).

#### 7. References

- [1] X. Weng, W. Cai, G. Owens, Z. Chen, Magnetic iron nanoparticles calcined from biosynthesis for fluoroquinolone antibiotic removal from wastewater, *J. Clean. Prod.*, 319 (2021) 128734. <https://doi.org/10.1016/j.jclepro.2021.128734>
- [2] A. Samadi-Maybodi, M. Nikou, Removal of sarafloxacin from aqueous solution by a magnetized metal-organic framework; Artificial neural network modeling, *Polyhedron J.*, 179 (2020) 114342. <https://doi.org/10.1016/j.poly.2019.114342>
- [3] Y. Ding, Z. Gao, H. Li, Real milk sample assisted selection of specific aptamer towards sarafloxacin and its application in the establishment of an effective aptasensor, *Sens. Actuators B Chem.*, 343 (2021) 130113. <https://doi.org/10.1016/j.snb.2021.130113>
- [4] W. Yan, Y. Xiao, W. Yan, R. Ding, S. Wang, F. Zhao, The effect of bioelectrochemical systems on antibiotics removal and antibiotic resistance genes: a review, *Chem. Eng. J.*, 358 (2019) 1421-1437. <https://doi.org/10.1016/j.cej.2018.10.128>
- [5] X. Wang, R. Yin, L. Zeng, M. Zhu, A review of graphene-based nanomaterials for removal of antibiotics from aqueous environments, *Environ. Pollut.*, 253 (2019) 100-110. <https://doi.org/10.1016/j.envpol.2019.06.067>
- [6] L. Wang, H. Jiang, H. Wang, P.L. Show, A. Ivanets, D. Luo, C. Wang, MXenes as heterogeneous fenton-like catalysts for removal of organic pollutants: A review, *J. Environ. Chem. Eng.*, (2022) 108954. <https://doi.org/10.1016/j.jece.2022.108954>
- [7] T.-t. Zhu, Z.-x. Su, W.-x. Lai, Y.-b. Zhang, Y.-w. Liu, Insights into the fate and removal of antibiotics and antibiotic resistance genes using biological wastewater treatment technology, *Sci. Total Environ.*, 776 (2021) 145906. <https://doi.org/10.1016/j.scitotenv.2021.145906>
- [8] S.A. Almodaresi, M. Mohammadrezaei, M. Dolatabadi, M.R. Nateghi, Qualitative analysis of groundwater quality indicators based on Schuler and Wilcox diagrams: IDW and Kriging models, *J. Environ. Health Sustain. Dev.*, 4 (2019) 903-912. <https://doi.org/10.18502/jehsd.v4i4.2023>
- [9] M.J. Ahmed, S.K. Theydan, Fluoroquinolones antibiotics adsorption onto microporous activated carbon from lignocellulosic biomass by microwave pyrolysis, *J. Taiwan Inst. Chem. Eng.*, 45 (2014) 219-226. <https://doi.org/10.1016/j.tic.2013.08.001>



- doi.org/10.1016/j.jtice.2013.05.014
- [10] L. Wang, D. Luo, J. Yang, C. Wang, Metal-organic frameworks-derived catalysts for contaminant degradation in persulfate-based advanced oxidation processes, *J. Clean. Prod.*, 375 (2022) 134118. <https://doi.org/10.1016/j.jclepro.2022.134118>
- [11] F. Ghourchian, N. Motakef-Kazemi, E. Ghasemi, H. Ziyadi, Zn-based MOF-chitosan-Fe<sub>3</sub>O<sub>4</sub> nanocomposite as an effective nano-catalyst for azo dye degradation, *J. Environ. Chem. Eng.*, 9 (2021) 106388. <https://doi.org/10.1016/j.jece.2021.106388>
- [12] N.M. Kazemi, A novel sorbent based on metal-organic framework for mercury separation from human serum samples by ultrasound assisted-ionic liquid-solid phase microextraction, *J. Environ. Anal.*, 2 (2019) 67-78. <https://doi.org/10.24200/amecj.v2.i03.68>
- [13] Z. He, X. Wang, Y. Luo, Y. Zhu, X. Lai, J. Shang, J. Chen, Q. Liao, Effects of suspended particulate matter from natural lakes in conjunction with coagulation to tetracycline removal from water, *Chemosphere*, 277 (2021) 130327. <https://doi.org/10.1016/j.chemosphere.2021.130327>
- [14] S. Ata, M. Feroz, I. Bibi, I.-u. Mohsin, N. Alwadai, M. Iqbal, Investigation of electrochemical reduction and monitoring of p-nitrophenol on imprinted polymer modified electrode, *Synth. Met.*, 287 (2022) 117083. <https://doi.org/10.1016/j.synthmet.2022.117083>
- [15] D.G. Kim, D. Choi, S. Cheon, S.-O. Ko, S. Kang, S. Oh, Addition of biochar into activated sludge improves removal of antibiotic ciprofloxacin, *J. Water Process. Eng.*, 33 (2020) 101019. <https://doi.org/10.1016/j.jwpe.2019.101019>
- [16] S. Sun, H. Yao, W. Fu, S. Xue, W. Zhang, Enhanced degradation of antibiotics by photo-fenton reactive membrane filtration, *J. Hazard. Mater.*, 386 (2020) 121955. <https://doi.org/10.1016/j.jhazmat.2019.121955>
- [17] F. Haftan, N. Motakef-Kazemi, The sorbent based on MOF-5 and its polyurethane nanocomposite for copper adsorption from aqueous solution, *J. Nanomed. Res.*, 6 (2021) 287-295. <https://doi.org/10.22034/NMRJ.2021.03.009>
- [18] A. Kausar, K. Naeem, M. Iqbal, Z.-i.-H. Nazli, H.N. Bhatti, A. Ashraf, A. Nazir, H.S. Kusuma, M.I. Khan, Kinetics, equilibrium and thermodynamics of dyes adsorption onto modified chitosan: a review, *Z Phys. Chem.*, (2021) 000010151520191586. <https://doi.org/10.1515/zpc-2019-1586>
- [19] R. Anjali, S. Shanthakumar, Insights on the current status of occurrence and removal of antibiotics in wastewater by advanced oxidation processes, *J. Environ. Manage.*, 246 (2019) 51-62. <https://doi.org/10.1016/j.jenvman.2019.05.090>
- [20] Z. Kang, X. Jia, Y. Zhang, X. Kang, M. Ge, D. Liu, C. Wang, Z. He, A review on application of biochar in the removal of pharmaceutical pollutants through adsorption and persulfate-based AOPs, *Sustainability*, 14 (2022) 10128. <https://doi.org/10.3390/su141610128>
- [21] N. Motakef kazemi, Zinc based metal-organic framework for nickel adsorption in water and wastewater samples by ultrasound assisted-dispersive-micro solid phase extraction coupled to electrothermal atomic absorption spectrometry, *J. Environ. Anal.*, 3 (2020) 5-16. <https://doi.org/10.24200/amecj.v3.i04.123>
- [22] J. Gu, J. Xie, S. Li, G. Song, M. Zhou, Highly efficient electro-peroxone enhanced by oxygen-doped carbon nanotubes with triple role of in-situ H<sub>2</sub>O<sub>2</sub> generation, activation and catalytic ozonation, *Chem. Eng. J.*, 452 (2023) 139597. <https://doi.org/10.1016/j.cej.2022.139597>
- [23] N. Dabuth, S. Thuangchon, T. Prasert, V. Yuthawong, P. Phungsai, Effects of catalytic ozonation catalyzed by TiO<sub>2</sub> activated carbon and biochar on dissolved organic matter removal and disinfection by-product

- formations investigated by Orbitrap mass spectrometry, *J. Environ. Chem. Eng.*, 10 (2022) 107215. <https://doi.org/10.1016/j.jece.2022.107215>
- [24] H. Pokkiladathu, S. Farissi, A. Muthukumar, M. Muthuchamy, A novel activated carbon-based nanocomposite for the removal of bisphenol-A from water via catalytic ozonation: Efficacy and mechanisms, *Results Chem.*, 4 (2022) 100593. <https://doi.org/10.1016/j.rechem.2022.100593>
- [25] H.N. Bhatti, Y. Safa, S.M. Yakout, O.H. Shair, M. Iqbal, A. Nazir, Efficient removal of dyes using carboxymethyl cellulose/alginate/polyvinyl alcohol/rice husk composite: adsorption/desorption, kinetics and recycling studies, *Int. J. Biol. Macromol.*, 150 (2020) 861-870. <https://doi.org/10.1016/j.ijbiomac.2020.02.093>
- [26] A. Bukhari, M. Atta, A. Nazir, M.R. Shahab, Q. Kanwal, M. Iqbal, H. Albalawi, N. Alwadai, Catalytic degradation of MO and MB dyes under solar and UV light irradiation using ZnO fabricated using *Syzygium Cumini* leaf extract, *Z Phys. Chem.*, 236 (2022) 659-671. <https://doi.org/10.1515/zpch-2021-3096>
- [27] M. Dolatabadi, H. Naidu, S. Ahmadzadeh, A green approach to remove acetamiprid insecticide using pistachio shell-based modified activated carbon; economical groundwater treatment, *J. Clean. Prod.*, 316 (2021) 128226. <https://doi.org/10.1016/j.jclepro.2021.128226>
- [28] R.A. Khera, M. Iqbal, A. Ahmad, S.M. Hassan, A. Nazir, A. Kausar, H.S. Kusuma, J. Niasr, N. Masood, U. Younas, Kinetics and equilibrium studies of copper, zinc, and nickel ions adsorptive removal on to *Archontophoenix alexandrae*: conditions optimization by RSM, *Desalin. Water Treat.*, 201 (2020) 289-300. <https://doi: 10.5004/dwt.2020.25937>
- [29] R. Huang, J. Yang, Y. Cao, D.D. Dionysiou, C. Wang, Peroxymonosulfate catalytic degradation of persistent organic pollutants by engineered catalyst of self-doped iron/carbon nanocomposite derived from waste toner powder, *Sep. Purif. Technol.*, 291 (2022) 120963. <https://doi.org/10.1016/j.seppur.2022.120963>
- [30] U.H. Siddiqua, S. Ali, T. Hussain, M. Iqbal, N. Masood, A. Nazir, Application of multifunctional reactive dyes on the cotton fabric and conditions optimization by response surface methodology, *J. Nat. Fibers*, 19 (2022) 1094-1106. <https://doi.org/10.1080/15440478.2020.1789532>
- [31] M. Yoosefian, E. Rahmanifar, N. Etminan, Nanocarrier for levodopa Parkinson therapeutic drug; comprehensive benserazide analysis, *Artif. Cells Nanomed. Biotechnol.*, 46 (2018) 434-446. <https://doi.org/10.1080/1691401.2018.1430583>
- [32] H. Raissi, A. Khanmohammadi, M. Yoosefian, F. Mollania, Ab initio and DFT studies on 1-(thionitrosomethylene) hydrazine: conformers, energies, and intramolecular hydrogen-bond strength, *Struct. Chem.*, 24 (2013) 1121-1133. <https://doi.org/10.1007/s11224-012-0144-6>
- [33] M.S. Thakur, N. Singh, A. Sharma, R. Rana, A.A. Syukor, M. Naushad, S. Kumar, M. Kumar, L. Singh, Metal coordinated macrocyclic complexes in different chemical transformations, *Coord. Chem. Rev.*, 471 (2022) 214739. <https://doi.org/10.1016/j.ccr.2022.214739>
- [34] M. Chandel, M. Thakur, A. Sharma, D. Pathania, A. Kumar, L. Singh, Chlorophyll sensitized (BiO)  $2\text{CO}_3/\text{CdWO}_4/\text{rGO}$  nano-hybrid assembly for solar assisted photo-degradation of chlorzoxazone, *Chemosphere*, 305 (2022) 135472. <https://doi.org/10.1016/j.chemosphere.2022.135472>
- [35] C. Mansas, J. Mendret, S. Brosillon, A. Ayrat, Coupling catalytic ozonation and membrane separation: A review, *Sep. Purif. Technol.*, 236 (2020) 116221. <https://doi.org/10.1016/j.seppur.2019.116221>
- [36] Y. Guo, J. Long, J. Huang, G. Yu, Y. Wang,

- Can the commonly used quenching method really evaluate the role of reactive oxygen species in pollutant abatement during catalytic ozonation, *Water Res.*, 215 (2022) 118275. <https://doi.org/10.1016/j.watres.2022.118275>
- [37] Z. Mohamad, A.A. Razak, S. Krishnan, L. Singh, A. Zularisam, M. Nasrullah, Treatment of palm oil mill effluent using electrocoagulation powered by direct photovoltaic solar system, *Chem. Eng. Res. Des.*, 177 (2022) 578-582. <https://doi.org/10.1016/j.cherd.2021.11.019>
- [38] G. Yu, Y. Wang, H. Cao, H. Zhao, Y. Xie, Reactive oxygen species and catalytic active sites in heterogeneous catalytic ozonation for water purification, *Environ. Sci. Technol.*, 54 (2020) 5931-5946. <https://doi.org/10.1021/acs.est.0c00575>
- [39] E. Issaka, J.N.-O. Amu-Darko, S. Yakubu, F.O. Fapohunda, N. Ali, M. Bilal, Advanced catalytic ozonation for degradation of pharmaceutical pollutants—A review, *Chemosphere*, 289 (2022) 133208. <https://doi.org/10.1016/j.chemosphere.2021.133208>